ICC
Iranian Chemical Communication
Original Research Article
Payame Noor University http://icc.journals.pnu.ac.ir

Kinetics of photocatalytic degradation of Methylene Blue by ZnO-bentonite nanocomposite

Sandip Pandurang Patil[a], Vilas Kailas Mahajan[b], Vinod Shankar Shrivastava[a], Gunvant Hari Sonawane[b]*

[a]*Nano-chemistry Research Laboratory, G. T. Patil College, Nandurbar-425 412 (M.S.), India*

[b]*Deptartment of Chemistry, Kisan Arts, Commerce and Science College, Parola-425 111(M.S.), India*

Received: 22 January 2017, Accepted: 16 August 2017, Published: 16 August 2017

Abstract

The present study reports the synthesis of ZnO-bentonite nanocomposite by the incorporation of ZnO with bentonite clay. The nanocomposite was characterised by XRD, SEM and EDS. ZnO-bentonite was effectively used for removal of Methylene Blue (MB). Removal of MB takes place by photocatalytic degradation and adsorption. Photocatalytic degradation of MB occurs by advanced oxidation process. The factors affecting photocatalytic degradation like pH, initial dye concentration, contact time and photocatalyst dose are investigated. Optimum pH was 8 and contact time was 80 min for photocatalytic degradation of MB. The kinetic study shows that adsorption follows pseudo-second-order kinetics. Adsorption was also described by Langmuir and Freundlich isotherms. Adsorption isotherm found to follow Langmuir isotherm. The monolayer coverage capacity was observed to be 62.5 mg/g. The amount of dye adsorbed was 252.7 mg/g for 0.2 g/L photocatalyst dose at 60mg/L MB concentration.

Keywords: Methylene Blue; photocatalytic degradation; ZnO-bentonite; advanced oxidation process.

Introduction

Dye production and textile manufacturing industries introduce large amount of wastewater containing different dyes and organics into the environment. Textile industries generate 100-170 L dye effluent per kg of processed cloth. Since dyes are stable, potentially carcinogenic and toxic, their release causes serious environmental problems [1,2]. It was observed that dyes show toxic effect as well as reduce light penetration in the contaminated water bodies. Most of the textile dyes are stable to the chemical oxidation and biodegradation [2,3]. Due to these characteristics dyes exhibit more resistivity towards decolourisation by conventional biochemical and physicochemical methods [4-6]. So to decrease the environmental issues, it is essential to remove these dyes before discharging effluent into the environment. In this context, several physical, chemical and biological techniques are reported for removal of these dyes [7,8].

Recently, extensive work has been carried out on semiconductor based photocatalysts due to their photoefficiency [9-10]. Semiconductor based nanocomposites are also found to

*Corresponding author: G.H. Sonawane
Tel: +91 (2597222441), Fax: +91 (2597223688)
E-mail: drgunvantsonawane@gmail.com

be efficient for the removal of different dyes and organics from wastewater. Many researchers have carried out a work on clay supported semiconductor nanocomposite [4,8]. Photocatalytic degradation and adsorption can be attributed to enhancement in removal efficiency of nanocomposites. Semiconductor photocatalysts like ZnO have more negative potential of electron derived from it, as compared to TiO_2. Thus ZnO is effectively used for photocatalytic degradation of organics from wastewater. Clay from the nanocomposite is responsible for adsorption [11,12], which is efficient and the most effective method for the removal of organics from wastewater, especially when the organic species are transferred from water effluent to solid phase [13-16]. Also due to the cost effectiveness and ease of operation adsorption has been found to be a promising method. The heterogeneous photocatalyst removes organic pollutants from industrial wastewater by Advanced Oxidation Processes [17,18].

The present study involves synthesis of nanocomposite using ZnO semiconductor, bentonite clay and characterization ZnO-bentonite. Photocatalytic degradation of MB was carried out using ZnO-bentonite nanocomposite; also experimental conditions are optimised for photocatalytic degradation of MB.

Experimental

Materials

Methylene Blue is a cationic dye with molecular weight 319.85 g/mol (M.F. $C_{16}H_{18}N_3SCl$). Stock solution (500mg/L) of Methylene Blue was prepared in distilled water. The experimental solutions of required concentrations are prepared by diluting stock solution with distilled water. All other chemicals used in this study were of analytical grade. The molecular structure of MB is shown in Figure 1.

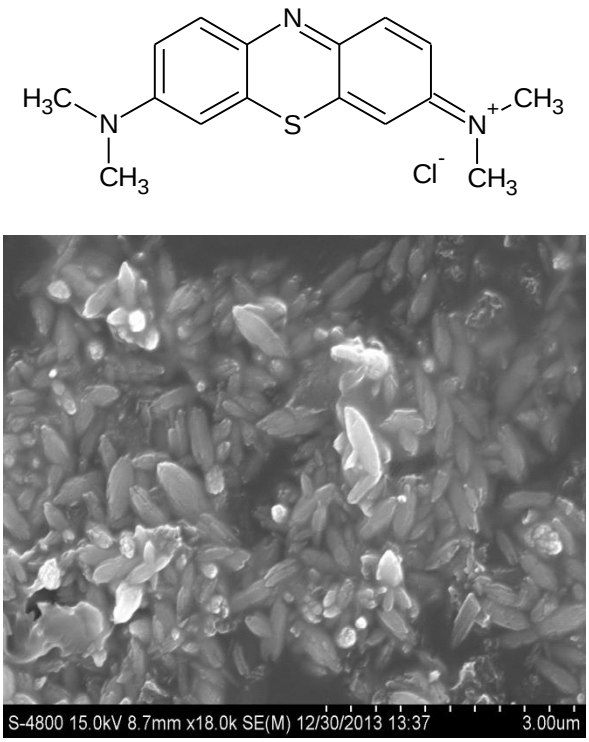

Figure 1. Molecular structure of the Methylene Blue

Synthesis of ZnO-Bentonite nanocomposite

Bentonite clay was purified as reported by Meshram et al [4]. ZnO-Bentonite nanocomposite was synthesized by intercalation of ZnO into the bentonite clay [4]. Initially, 2 g $Zn(CH_3COO)_2{\cdot}2H_2O$ was dissolved in 250 mL DMF, to which 10 g purified clay was added. Then the mixture was sonicated for 3h to obtain homogeneous suspension. To this solution, 100 mL of 0.1 M NaOH solution was added with continuous stirring for 1 h. The nanocomposite was obtained after successive centrifugation and dispersions in alcohol. Finally nanocomposite was dried under vacuum and calcinated at 200 ^{0}C for 2-3 h.

Photocatalytic study

The photocatalytic degradation of MB was carried out in photocatalytic reactor, containing 400 W mercury lamp. Cooling water jacket is used to maintain the inside temperature of the reactor. 50 mL dye solution having different nanocomposite doses were placed in a photocatalytic reactor, then adequate amount of the sample was withdrawn at regular intervals. After centrifugation, changes in dye concentration were determined by UV-visible double beam spectrophotometer (Systronics model-2203) at λ_{max} 664nm. The removal percentage of MB and the amount of MB adsorbed were calculated by equations 1 and 2.

$$\boldsymbol{Removal\ percentage} = \left(\frac{C_i - C_t}{C_i}\right) \mathbf{100} \quad (1)$$

$$q_t = \frac{(C_i - C_t)V}{W} \quad (2)$$

where C_i (mg/L) is the initial MB dye concentration; C_t (mg/L) is the MB concentration at time t ; q_t (mg/g) is the adsorption capacity at time t; V (L) is the initial volume of dye solution and W (g) is the amount of nanocomposite.

Result and discussion

SEM and EDS analysis

Scanning electron microscopy was used to study the morphology of ZnO-bentonite. Figure 2 (a) shows the SEM of ZnO-bentonite nanocomposite. SEM micrograph shows that ZnO-bentonite has well defined granular particle size having grooves favourable for photodegradation and adsorption. Figure 2 (b) shows that ZnO-bentonite contains C K (21.33%), O K(33.37%), Zn K(11.34%), Na K(1.40%), Si K(24.81%), Fe K(0.91%), Al K(2.64%),and Ca K(0.20%). EDS of ZnO-bentonite micrograph shows the presence of peaks of Zn and O proves existence of ZnO in the nanocomposite.

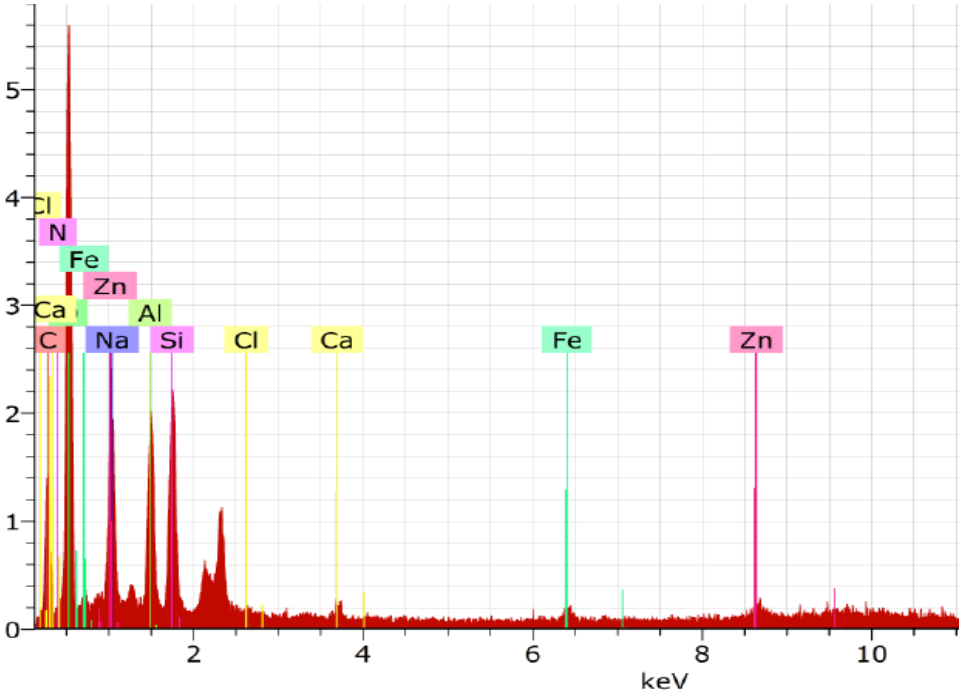

Figure 2. SEM micrograph (a) and EDS (b) of ZnO-bentonite

X-ray diffraction analysis

The XRD diagram of ZnO-bentonite is shown in Figure 3. The prominent ZnO peaks observed at 2θ of 30.9°, 33.5°, 35.3°and 55.7°are attributed to (1 0 0), (0 0 2), (1 0 1), and (1 1 0) planes respectively [4] (JCPDS Card No.75-1533). Natural bentonite peak was observed at 2θ of 25.7°.

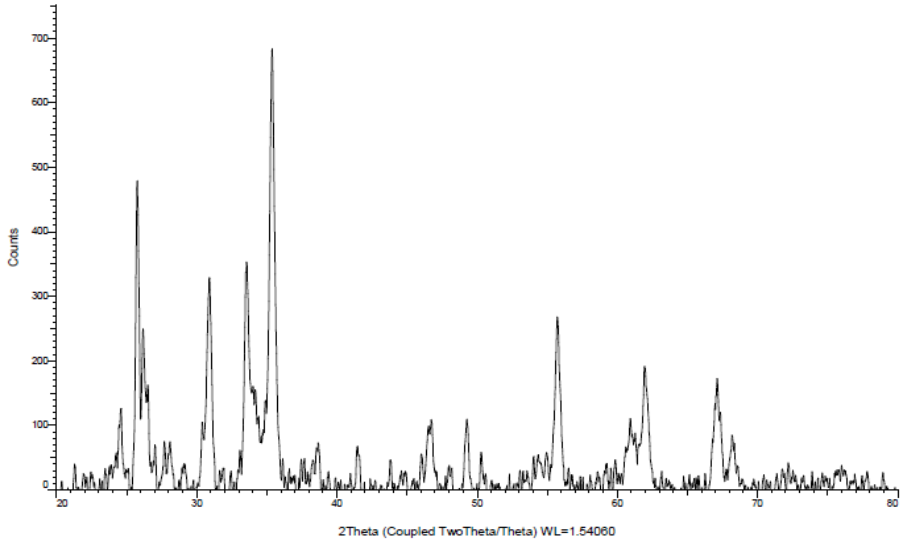

Figure 3. XRD of ZnO-bentonite

Effect of pH

Photocatalytic degradation of dye is greatly influenced by pH of the dye solution. The effect of pH on photocatalytic degradation was studied from pH 1 to 10 at 20 mg/L MB concentration for 1g/L ZnO-bentonite dose. It was observed that initially percentage removal increases from 77 to 89.9% as pH increases from 1 to 8

then thereafter it decreases upto 87.8%. Since MB is a cationic dye, its degradation and adsorption are favoured at higher pH due to the more availability of ^{-}OH to generate more $^{\bullet}OH$ radicals. $^{\bullet}OH$ radicals are responsible for photodegradation of MB [19-21]. Further, increasing the pH resulted into a decrease in the rate of photocatalytic degradation. The present study reports the higher probability of occurrence of degradation of MB at surface of ZnO-bentonite nanocomposite. After a certain pH value, more $O_2^{-\bullet}$ are generated that will make the surface of semiconductor negatively charged and it restricts the approach of dye molecules towards the semiconductor surface. This will result into a decrease in the rate of photocatalytic degradation of MB.

Effect of contact time and initial dye concentration

Removal of dye from wastewater depends on initial dye concentration and contact time. The effect of initial dye concentration and contact time on removal of MB by ZnO-bentonite is shown in Figure 4. It was found that, initially the dye removal is faster then it becomes slower to attain equilibrium. The equilibrium time was found to be 80 min. As dye concentration increases from 20 to 60 mg/L, the percentage removal decreases from 97.3 to 97.1% for 1g/L photocatalyst dose. Initially the amount of dye adsorbed on ZnO-bentonite nanocomposite increases with increase in dye concentration, then thereafter it attains equilibrium (Figure 5). The amount of adsorbed dye (q_t) increases from 19.46 to 58.78 mg/g when dye concentration was increased from 20 to 60 mg/L for 1g/L photocatalyst dose. The adsorption was pre-conducted in dark for 60 min for the dye solution in the presence of catalysts. The absorbability of ZnO, bentonite and ZnO-bentonite are 9.5, 24.3 and 38.5% respectively for 20 mg/L MB concentration and 1 g/L of catalyst. After light irradiation upto 80 min, 57.4, 27.7 and 97.3% MB were degraded by photocatalysis using ZnO, bentonite and ZnO-bentonite respectively (Figure 6). However, blank study shows the stability of the dye in presence of light only.

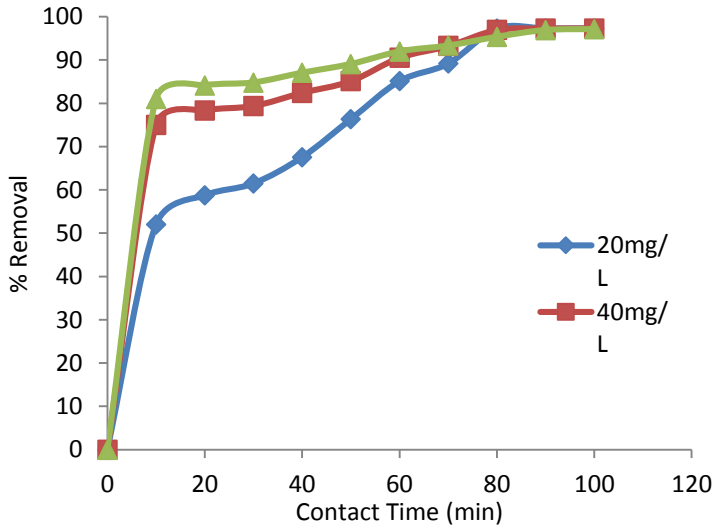

Figure 4. Effect of contact time and initial concentration of MB on percent removal; pH 8, Photocatalyst dose 1g/L

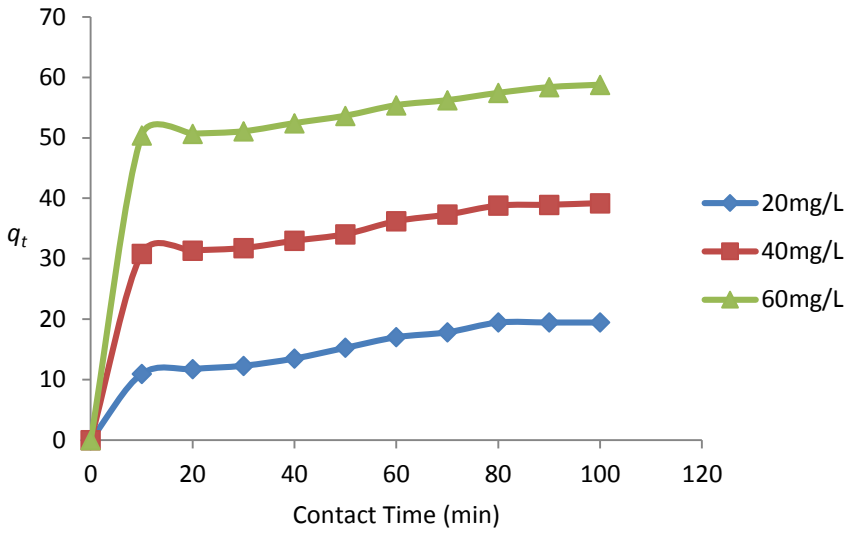

Figure 5. Amount of dye adsorbed q_t (mg/g) with time for different initial dye concentration; pH 8, photocatalyst dose 1 g/L

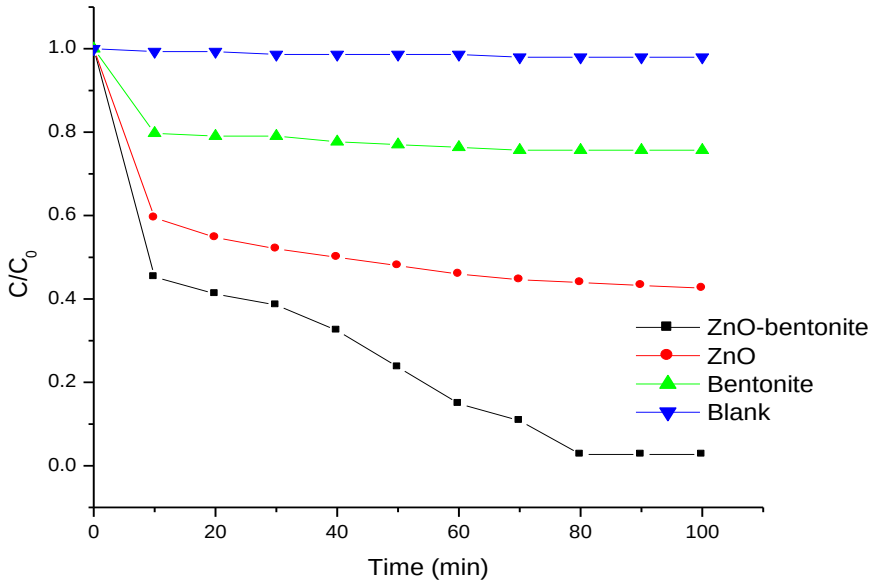

Figure 6. Photocatalytic performance of ZnO, bentonite and ZnO-bentonite (1g/L) for degradation of MB (20mg/L)

Recycle study

Stability of the nanocomposite was confirmed by recycle study. The powdered nanocomposite was allowed to settle after the photocatalytic degradation. The nanocomposite was then collected and reused for 2 times under same photodegradation conditions. Figure 7 shows removal of MB by ZnO-bentonite. After the 1st run MB degraded upto 97.3%. After the 2nd and 3rd run, removal of MB decreases down to 93.2 and 90.5%. Loss of the recycled catalyst during sampling is responsible for decrease in the removal of MB.

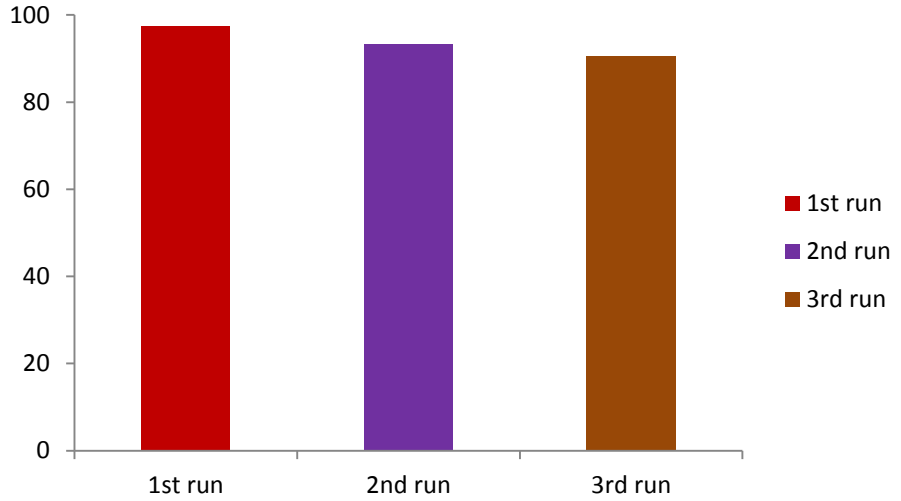

Figure 7. Recycle study of ZnO-bentonite (1g/L) for degradation of MB (20mg/L)

From Table 1 it was concluded that MB removal by ZnO-bentonite was an efficient method in comparison to various removal efficiencies, operational times and initial dye concentrations of similar studies in the literature.

Table 1. MB removal efficiencies (%) of various methods

Nanomaterial	Removal efficiency (%)	Operation time (min)	Sources
ZnS:CdS	73	360	[22]
Fe doped TiO_2	94	120	[23]
TiO_2/activated carbon	98	90	[24]
ZnO-bentonite	97.3	80	This study

Effect of photocatalyst dose

Capacity of photocatalyst to remove dye depends on photocatalyst dose. The effect of photocatalyst dose on dye removal was studied under constant experimental conditions. The removal percentage of MB by ZnO-bentonite at different photocatalyst doses 0.2 to 2 g/L for 20 to 60 mg/L dye concentration was studied. Figure 8 shows the effect of photocatalyst dose on amount of adsorbed dye. The amount of adsorbed dye (q_t) increases from 20 to 60 mg/L for 0.2 g/L photocatalyst dose. Figure 8 shows that, as adsorbent mass increases, there is considerable increase in amount of adsorbed dye but amount of adsorbed per unit mass of adsorbent decreases. As photocatalyst dose increases from 0.2 to 2 g/L, the amount of adsorbed dye (q_t) decreases from 252.7 to 29.66 mg/g, while percentage removal increases from 83.9 to 98.5%.

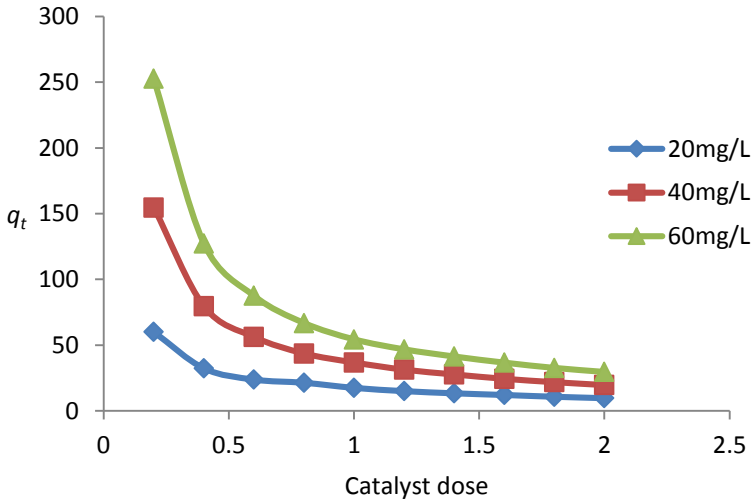

Figure 8. Amount of dye adsorbed q_t (mg/g) with photocatalyst dose (g/L) for different initial concentrations, contact time 80 min, pH 8

Adsorption kinetics

Mechanism and efficiency of adsorption is given by adsorption kinetics. Adsorption kinetics of MB on ZnO-bentonite was studied with the help of pseudo-first-order and pseudo-second-order.

The pseudo-first-order model

A linear form of pseudo-first-order kinetics described by Lagergren [8,25] was given by Eq. 3:

$$\log(q_e - q_t) = \log q_e - \frac{K_1 t}{2.303} \quad (3)$$

where q_e and q_t are the amount of dye adsorbed (mg/g) on ZnO-bentonite at equilibrium and at time t respectively; K_1 is the first order adsorption rate constant (min^{-1}) given by plot of $\log(q_e - q_t)$ vs t. Validity of Lagergren equation was given by linearity of the plot. The calculated K_1 and co-relation coefficient r^2 values are shown in Table 2. The smaller r^2 values ($r^2 < 0.947$) and calculated q_e values from pseudo-first-order kinetics compared to experimental q_e values indicates inapplicability of pseudo-first-order kinetics to predict adsorption kinetics of MB on ZnO-bentonite.

Table 2. Comparison of adsorption rate constants, calculated and experimental q_e values for different initial dye concentrations and photocatalyst dose for different kinetic models

Adsorbent g/L	Dye concentration mg/L	Pseudo first-order			
		q_e(exp) (mg/g)	K_1 min^{-1}	q_e(cal) (mg/g)	r^2
1	20	19.46	0.0276	14.19	0.908
	40	38.78	0.0253	13.52	0.858
	60	57.43	0.0276	12.65	0.875
2	20	9.73	0.0760	4.84	0.925
	40	19.73	0.0691	19.14	0.947
	60	28.99	0.0322	6.64	0.861
Adsorbent g/L	**Dye concentration mg/L**	**Pseudo second-order**			
		K_2x10^{-3}g/mg min	q_e(cal) (mg/g)	h	r^2

1	20	1.906	23.80	1.079	0.968
	40	3.114	41.66	5.405	0.993
	60	3.325	62.50	12.987	0.997
2	20	0.046	10.00	4.651	0.999
	40	9.766	20.83	4.237	0.999
	60	6.966	31.25	6.803	0.997

The pseudo-second-order model

The amount of solute adsorbed on adsorbent surface and the amount adsorbed at equilibrium describes the rate of pseudo-second-order reaction. The pseudo-second-order model [16,26] is expressed by Eq. 4:

$$\frac{t}{q_t} = \frac{1}{K_2 q_e^2} + \frac{t}{q_e} \quad \text{and} \quad h = K_2 q_e^2 \qquad (4)$$

where K_2 is second-order adsorption rate constant (g mg^{-1} min^{-1}), h is the initial rate (mg g^{-1} min), which are given by slope and intercept of plot of t/q_t vs t (Figure 9). The linearity of the plot with higher co-relation coefficient r^2 (0.968-0.999) indicates good agreement of calculated q_e values with experimental q_e values (Table 2). This shows that adsorption kinetics follows pseudo-second-order kinetics.

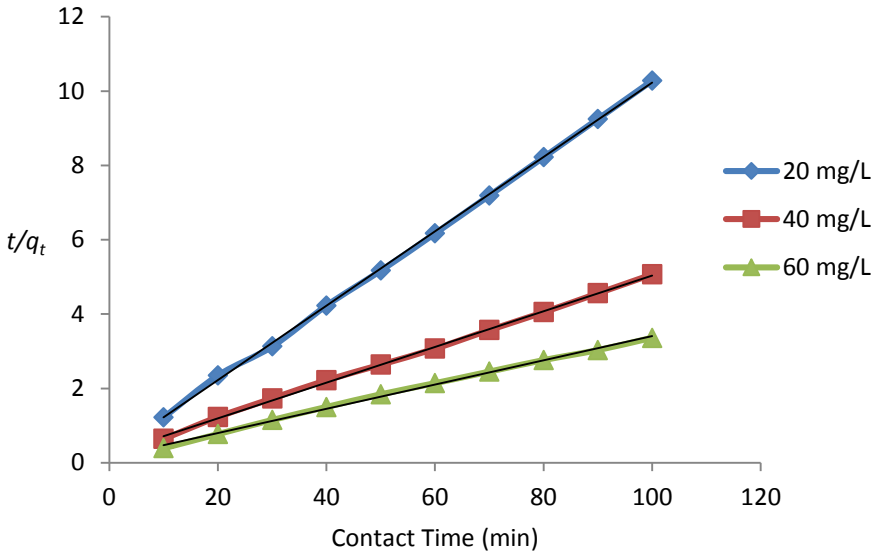

Figure 9. Second order kinetics plots for the removal of MB at different initial dye concentrations; photocatalyst dose 2 g/L, pH 8

Adsorption isotherms

Freundlich isotherm model

Freundlich Isotherm describes non-ideal, reversible, multilayer adsorption. Linear form of Freundlich Isotherm [27] is given by Eq. 5:

$$\log q_e = \log K_F + \frac{1}{n} \log C_e \qquad (5)$$

where q_e is amount of adsorbed dye per unit mass of adsorbent (mg/g); K_F is Freundlich isotherm constant (mg/g) $(L/g)^n$; $1/n$ is a measure of adsorption density; C_e is equilibrium concentration of dye. Figure 10 shows the linear nature of plot of *log* q_e vs *log* C_e which indicates the adsorption isotherm following Freundlich isotherm. Freundlich isotherm is widely applied to heterogeneous systems. If the slope

(*1/n*) = 1, adsorption is linear; if *1/n* < 1, chemisorption and adsorption is favourable; if *1/n* > 1, co-operative adsorption [28]. The *1/n* values between 0.332 to 0.49 for 20 to 60 mg/L dye concentration indicates that adsorption is favorable, and it is a chemisorption process. The slope (*1/n*) and K_F values are presented in Table 3.

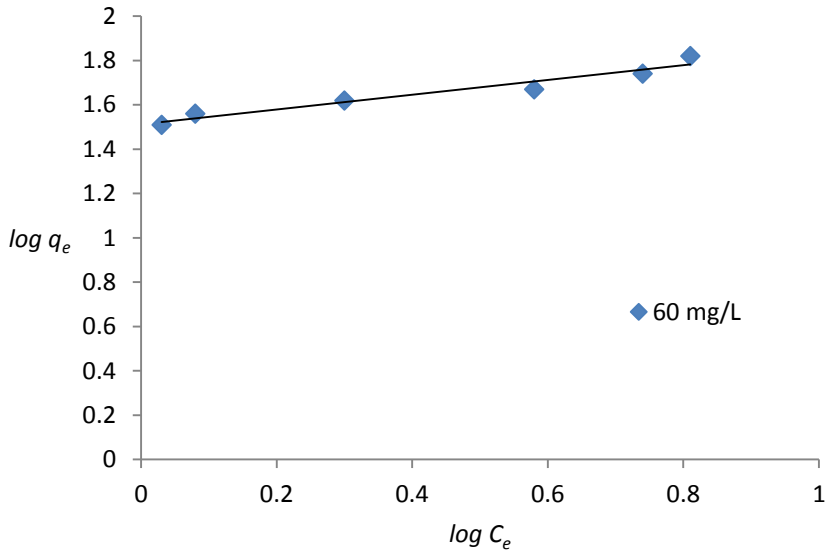

Figure 10. Freundlich plot for adsorption of MB by ZnO-bentonite

Table 3. Freundlich and Langmuir isotherm constants for adsorption of MB on ZnO-bentonite for different dye concentration and photocatalyst dose of 0.2 to 2 g/L at pH 8, contact time 80 min

Dye concentration mg/L	**Freundlich coefficient**				**Langmuir coefficient**			
	K_F **(L/g)**	***n***	***1/n***	r^2	***a* (mg/g)**	***b* (g/L)**	R_L	r^2
20	11.88	2.1277	0.47	0.932	27.77	0.9730	0.0489	0.969
40	23.17	2.0408	0.49	0.867	50.00	1.1765	0.0208	0.980
60	32.51	3.0120	0.33	0.943	62.50	1.1429	0.0144	0.991

Langmuir isotherm model

Langmuir model assumes homogeneous monolayer adsorption. Langmuir isotherm related to rapid decrease of the intermolecular attractive forces to the rise of the distance. The linear form of Langmuir isotherm [27] is given by Eq. 6:

$$\frac{C_e}{q_e} = \frac{1}{ab} + \frac{C_e}{a} \qquad (6)$$

where *a* is monolayer coverage capacity (mg/g) and *b* is Langmuir isotherm constant (L/mg). Figure 11 shows linear nature which indicates, adsorption following Langmuir isotherm. Langmuir isotherm suggests the monolayer coverage of MB on ZnO-bentonite. The calculated *a* and *b* values are presented in Table 3. Weber and Chakkravorti express the Langmuir isotherm by dimensionless factor R_L, which is given by Eq. 7:

$$R_L = \frac{1}{1+bC_i} \qquad (7)$$

The nature of adsorption is given by R_L i.e. separation factor. When R_L = 0, adsorption is irreversible; 1 > R_L > 0, adsorption is favourable; R_L = 1,

adsorption is linear and $R_L > 1$, adsorption is unfavourable. The present study reports lower R_L values ($1 > R_L > 0$) indicates adsorption is favourable.

The higher co-relation coefficient r^2 values indicate that adsorption of MB on ZnO-bentonite nanocomposite found to follow Langmuir isotherm.

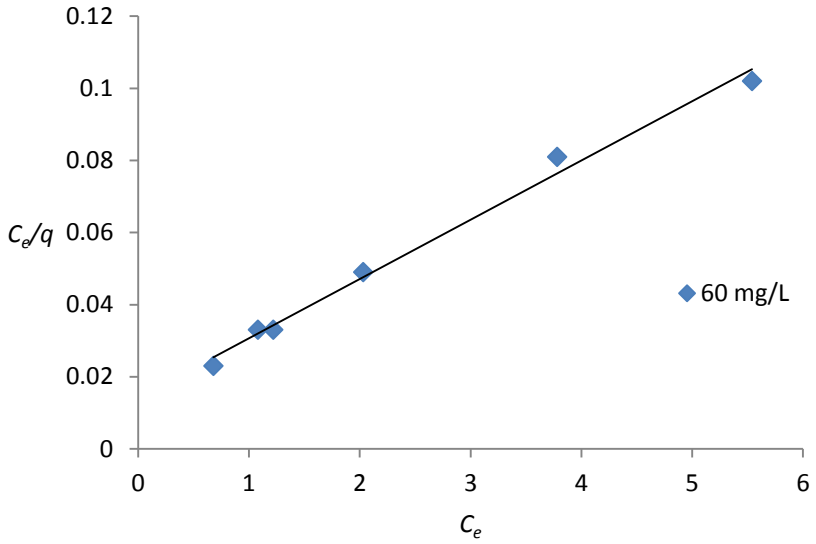

Figure 11. Langmuir plot for adsorption of MB by ZnO-bentonite

Conclusion

The experimental results show that removal of MB from aqueous solution by ZnO-bentonite was found to be a promising method. The amount of adsorbed dye (q_t) was affected by contact time, pH, initial dye concentration and photocatalyst dose. The removal was favoured at pH 8. The equilibrium time was found to be 80min. The amount of adsorbed dye increases with increase in contact time, initial dye concentration and decreases with increase in photocatalyst dose. q_t value decreases from 252.7 to 29.66 mg/g as photocatalyst dose increases from 0.2 to 2 g/L. The adsorption kinetics found to follow pseudo-second-order kinetics. Due to the higher co-relation coefficient r^2 values Langmuir isotherm fits well with experimental data than Freundlich isotherm. The dimensionless factor (R_L) indicates that ZnO-bentonite can be effectively used for removal of MB from aqueous solution. Recycle study indicates the stability of the ZnO-bentonite nanocomposite.

Acknowledgments

The authors have gratefully acknowledged to Central Instrumentation Centre, University Institute of Chemical Technology, NMU, Jalgaon for SEM and XRD analysis. Authors are also thankful to Principal, Kisan College, Parola and Principal, GTP College, Nandurbar for providing necessary laboratory facilities.

References

[1] B. H. Hameed, R.R. Krishni, S.A. Sata, *J. Hazard. Mater.*, **2009**, 162, 305–311.
[2] G.L.J. Zhao, *New J. Chem.*, **2000**, 24, 411-417.
[3] I. Arslan, A.I. Balcioglu, *J. Chem. Technol. Biotechnol.*, **2001**, 76, 53–60.
[4] S. Meshram, R. Limaye, S. Ghodke, S. Nigam, S. Sonawane, R.

Chikate, *Chem. Eng. J.*, **2011**, 172, 1008-1015.
[5] W. Dong, C.W. Lee, X. Lu, Y. Sun, W. Hua, G. Zhuang, S. Zhang, J. Chen, H. Hou, D. Zhao, *Appl. Catal. B*, **2010**, 95, 197–207.
[6] D.P. Tiwari, S.K. Singh, N. Sharma, *Appl. Water Sci.*, **2015**, 5, 81-88.
[7] H.S. Kibombo, R. Peng, S. Rasalingam, R.T. Koodali, *Catal. Sci. Technol.*, **2012**, 2, 1737–1766.
[8] S.P. Patil, V.S. Shrivastava, G.H. Sonawane, *Desalin. Water Treat.*, **2015**, 54, 374-381.
[9] R. Georgekutty, M.K. Seery, S.C. Pillai, *J. Phys. Chem. C*, **2008**, 112, 13563–13570.
[10] U.G. Akpan, B.H. Hameed, *J. Hazard. Mater.*, 2009, 170, 520–529.
[11] Y.H. Son, J.K. Lee, Y. Soong, D. Martello, M. Chyu, *Chem. Mater.*, **2010**, 22, 2226–2232.
[12] S. Sonawane, P. Chaudhari, S. Ghodke, S. Phadtare, S. Meshram, *J. Sci. Ind. Res.*, **2009**, 68, 162–167.
[13] M. Hajjaji, A. Beraa, *Appl. Water Sci.*, 2015, 5, 71-79.
[14] E. Bazrafshan, A.A. Zarei, H. Nadi, M.A. Zazouli, *Ind. J. Chem. Tech.*, **2014**, 21, 105-113.
[15] Q. Wang, C. Chen, D. Zhao, W. Ma, J. Zhao, *Langmuir*, **2008**, *24*, 7338-7345.
[16] M.-C. Shih, *Desalin. Water Treat.*, **2012**, 37, 200-214.
[17] A. Di Paola, E. García-López, G. Marcì, L. Palmisano, *J. Hazard. Mater.*, **2012**, 211– 212, 3– 29.
[18] M. Safari, M. Nikazar, M. Dadvar, *J. Ind. Eng. Chem.*, **2013**, 19, 1697–1702.
[19] C.H. Guillard, H. Lachheb, A. Houas, M. Ksibi, E. Elaloui, J.M. Herrmann, *J. Photochem. Photobiol. A: Chem.*, **2003**, 158, 27.
[20] K. Bubacz, J. Choina, D. Dolat, A.W. Morawski, *Polish J. Environ. Stud.*, ***2010***, 19, (4) 685-691.
[21] Swati, Munesh & Meena R C, *Archives of Applied Science Research*, **2012**, 4 (1) 472-479.
[22] N. Soltani, E. Saion, M. Z. Hussein, M. Erfani, A. Abedini, G. Bahmanrokh, M. Navasery, P. Vaziri, *Int. J Mol. Sci.*, **2012**, 13, 12242-12258.
[23] Ö. Kerkez, İ Boz, *Reaction Kinetics, Mechanisms & Catalysis*, **2013**, 110, 543-557.
[24] Z.A.C. Ramli, N. Asim, W.N.R.W. Ishak, Z. Emdadi, N.A.-Ludin, M.A. Yarmo, K. Sopian, *The Scientific World Journal*, **2014**, 2014, 1-8.
[25] Y.S. Ho, G. McKay, *Resources, Conservation and Recycling*, **1999**, 25, 171–193.
[26] G.H. Sonawane, V.S. Shrivastava, *Desalination*, **2009**, 247, 430-441.
[27] K.Y. Foo, B.H. Hameed, *Chem. Eng. J.*, **2010**, 156, 2–10.
[28] F. Haghseresht, G. Lu, *Energy Fuels*, **1998**, 12, 1100–1107.